






Constraining Black Hole Populations in Globular Clusters Using Microlensing: Application to Omega Centauri

John Zaris¹, Doğa Veske¹ , Johan Samsing², Zsuzsa Márka³, Imre Bartos⁴ , and Szabolcs Márka¹ 

¹ Department of Physics, Columbia University in the City of New York, 550 W 120th St., New York, NY 10027, USA; jcz2114@columbia.edu

² Niels Bohr International Academy, The Niels Bohr Institute, Blegdamsvej 17, DK-2100, Copenhagen Ø, Denmark

³ Columbia Astrophysics Laboratory, Columbia University in the City of New York, 550 W 120th St., New York, NY 10027, USA

⁴ Department of Physics, University of Florida, P.O. Box 118440, Gainesville, FL 32611-8440, USA

Received 2020 January 30; revised 2020 April 13; accepted 2020 April 16; published 2020 May 1

Abstract

We estimate the rate of gravitational microlensing events of cluster stars due to black holes (BHs) in the globular cluster NGC 5139 (ωCen). Theory and observations both indicate that ωCen may contain thousands of BHs, but their mass spectrum and exact distribution are not well constrained. In this Letter we show that one may observe microlensing events on a timescale of years in ωCen , and such an event sample can be used to infer the BH distribution. Direct detection of BHs will, in the near future, play a major role in distinguishing binary BH merger channels. Here we explore how gravitational microlensing can be used to put constraints on BH populations in globular clusters.

Unified Astronomy Thesaurus concepts: [Black holes \(162\)](#); [Globular star clusters \(656\)](#); [Gravitational microlensing \(672\)](#)

1. Introduction

The detection of gravitational waves (GWs) by Advanced LIGO (Aasi et al. 2015) and Advanced Virgo (Acernese et al. 2015) has confirmed the existence of merging binary black holes (BBHs; Abbott et al. 2016a, 2016b, 2016c, 2017a, 2017b; Venumadhav et al. 2019; Zackay et al. 2019). However, there is limited evidence to explain how and where this observed BBH population forms in our universe. The growing list of proposed formation channels includes field binaries (Dominik et al. 2012; Belczynski et al. 2016; Mapelli et al. 2017; Murguía-Berthier et al. 2017; Silsbee & Tremaine 2017; Giacobbo & Mapelli 2018; Rodríguez & Antonini 2018; Schröder et al. 2018; Spera et al. 2019), active galactic nuclei disks (Bartos et al. 2017; McKernan et al. 2018; Stone et al. 2017; Yang et al. 2019), galactic nuclei (O’Leary et al. 2009; Hong & Lee 2015; Antonini & Rasio 2016; Stephan et al. 2016; VanLandingham et al. 2016; Hamers et al. 2018; Fragione et al. 2019), and dynamical assembly in globular clusters (GCs; Portegies Zwart & McMillan 2000; Banerjee et al. 2010; Ziosi et al. 2014; Mapelli 2016; Rodríguez et al. 2016a; Askar et al. 2017; Park et al. 2017; Fragione & Kocsis 2018; Antonini & Gieles 2020; Di Carlo et al. 2019). In this work we study methods to constrain the black holes (BH) population in GCs independently of GW observations.

Recently, BH candidates have been detected in GCs using a variety of methods, including analysis of X-ray and radio emissions (Strader et al. 2012; Chomiuk et al. 2013; Miller-Jones et al. 2015) and radial velocity measurements of BH companion stars in binary systems (Giesers et al. 2018, 2019). Stellar-mass BH candidates have even been found in GCs outside of the Milky Way by analyzing X-ray emission patterns (Maccarone et al. 2007, 2011; Brassington et al. 2010; Shih et al. 2010).

Theory and observations indicate that individual GCs are able to retain a large fraction of their initial BH population, depending on their mass and dynamical history (e.g., Morscher

et al. 2015; Rodríguez et al. 2016a; Askar et al. 2018; Kremer et al. 2018; Weatherford et al. 2019; Zocchi et al. 2019). One way of probing this population is through GW observations, but distinguishing BBHs mergers assembled in GCs from those formed through other channels has been shown to be difficult. Using inferred distributions of BH spins (e.g., Rodríguez et al. 2016b), masses (e.g., Zevin et al. 2017), and orbital eccentricities (e.g., Gültekin et al. 2006; Samsing et al. 2014, 2018a, 2018b, 2019; Samsing & Ramirez-Ruiz 2017; Samsing 2018; Samsing & Ilan 2018, 2019; Romero-Shaw et al. 2019; Zevin et al. 2019) from GW observations is possible, but gives only an indirect and statistical measure of the contribution of GC BBHs to the set of observed BBH mergers.

In this Letter, we explore the possibility of directly constraining the BH population of GCs located in the Milky Way (MW) through their gravitational lensing effects (e.g., Paczynski 1994; Udalski et al. 1994; Bennett et al. 2002). If BHs populate the core of GCs, then they will occasionally gravitationally lens and magnify the background cluster stars, an effect known as microlensing (e.g., Paczynski 1986).

Previous microlensing studies have investigated several types of lens-source systems. For example, research has been conducted on the lensing of galactic center stars by GC stars (Paczynski 1994; Pietrukowicz et al. 2012), planetary-mass objects (Sahu et al. 2001) and dark matter (Jetzer et al. 1998), and the lensing of GC stars by galactic compact dark matter (Rhoads & Malhotra 1998) and intermediate-mass BHs theorized to inhabit GCs (Safonova & Stalin 2010).

In this work, we study the microlensing of GC stars by stellar-mass GC BHs, focusing our attention on the massive GC ωCen . Recent studies indicate that a BH population with total mass $\sim 10^5 M_\odot$ is likely to occupy the core of ωCen (Zocchi et al. 2019), which makes this cluster a particularly interesting candidate to monitor in current and future surveys. Using both analytical and numerical techniques we illustrate that an observable microlensing rate $\sim 1 \text{ yr}^{-1}$ is expected for ωCen and investigate how this rate depends on the properties of the

BH population. Any detection or nondetection can therefore be used to constrain the current BH distribution in ωCen . This, in turn, can help determine the degree to which GCs contribute to the observed BBH merger rate.

The Letter is structured as follows. We begin in Section 2 by applying microlensing theory to the case of a GC, from which we derive an order-of-magnitude estimate for the lensing rate in ωCen . In Section 3 we improve on our rate estimate using a more sophisticated Monte Carlo (MC) technique, where we take into account the observed stellar profile of ωCen . We conclude our study in Section 4.

2. Lensing Theory and Toy Model

Here, we first review the standard lensing equations (e.g., Paczynski 1986), which we then use to derive an approximate but closed form expression for the rate of stellar microlensing by BHs in GCs. This expression provides general insight into how the microlensing rate depends on properties such as the mass and velocity dispersion of both the BH and star distributions.

When a lensing object (the BH) passes near the line of sight (LOS) from an observer to a source (the star), the source will appear magnified in the observer's frame by a factor

$$\mu = \frac{\alpha^2 + 2}{\alpha(\alpha^2 + 4)^{1/2}}, \quad (1)$$

where α is the rescaled angular impact parameter defined by

$$\alpha = \beta/\theta_E. \quad (2)$$

In this equation, β is the angular distance between the lensed star and the BH, and θ_E is the angular Einstein radius defined by

$$\theta_E = \sqrt{\frac{4Gm_{\text{BH}}}{c^2} \frac{D_S - D_L}{D_S D_L}}, \quad (3)$$

where D_S and D_L are the distances from the observer to the lensed star and to the BH, respectively, m_{BH} is the mass of the lensing BH, G is Newton's gravitational constant, and c is the speed of light. Figure 1 illustrates this setup.

Using these equations, we now derive an expression for the rate of microlensing in a GC consisting of stars and BHs. We begin by calculating the rate at which stars located in the source plane (S-plane) cross the Einstein ring of a given BH located in the lens plane (L-plane), where the radii of the Einstein rings in the L-plane and the S-plane are given by $R_L \approx D_L \theta_E$ and $R_S \approx D_S \theta_E$, respectively. Defining r as the distance between the two planes, it follows that the rate at which stars in the S-plane from r to $r + dr$ pass through the Einstein ring is given by

$$d\Gamma \approx 2n(r)R_S w dr, \quad (4)$$

where $n(r)$ is the density of stars in the S-plane at distance r , and w is the velocity dispersion of the stars relative to the Einstein ring in the S-plane. Note here that we have ignored the curvature of the S-plane, which is a valid approximation as $\theta_E \ll 1$. The relative velocity dispersion can be expressed as $w^2 = v_S^2 + (D_S/D_L)^2 u_L^2$, where v_S is the velocity dispersion of the stars in the S-plane and u_L is the velocity dispersion of the lensing BHs in the L-plane. Since $D_L \gg r$ we have that $R_S \approx R_L$, and $w^2 \approx v_S^2 + u_L^2 \approx u_L^2$, where the last

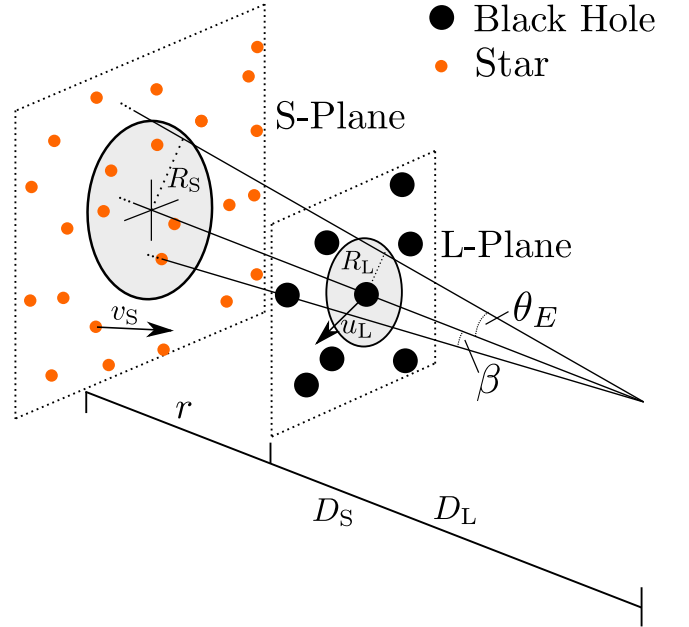


Figure 1. Illustration of the lensing setup described in Section 2. The illustration shows two planes: the source plane (S-Plane), which here is populated with stars (orange dots), and the lensing plane (L-Plane), which is populated with BHs (black dots). The observer is located to the right at a distance D_L and D_S to the L-Plane and S-Plane, respectively. The rate at which stars in the S-Plane cross the Einstein ring (gray circle in the S-Plane with radius R_S) is linked to the observable microlensing rate, as further described in Section 2.

approximation is accurate within a factor of unity depending on the stellar velocity profile, and on the degree to which the BHs are in energy equipartition with the stars (e.g., Kocsis et al. 2006; Trenti & van der Marel 2013). Generally, the BHs are located near the center of the GC as they are individually much heavier than the stars. Therefore, their velocity dispersion is $u_L \approx v_0$, where v_0 is the central value. With these approximations, the differential microlensing rate per BH lens can be written as

$$d\Gamma \approx 2n(r)D_L \theta_E v_0 dr. \quad (5)$$

Expressing the Einstein angle as $\theta_E = \sqrt{2\mathcal{R}r/D_L^2}$, where \mathcal{R} is the Schwarzschild radius of a BH with mass m_{BH} , Equation (5) can also be written as $d\Gamma = \sqrt{8}n(r)\sqrt{\mathcal{R}}\sqrt{r}v_0 dr$. This is the rate for stars in an infinitesimally thin slab located at a distance $(r, r + dr)$ from the L-plane, assuming one BH. Therefore, the total rate for a GC with N_{BH} BHs is given by

$$\Gamma \approx \sqrt{8}N_{\text{BH}}n_0\mathcal{R}^2v_0\left(\frac{R_{\text{GC}}}{\mathcal{R}}\right)^{3/2}\int n'\sqrt{r'}dr', \quad (6)$$

where $n' = n/n_0$ is the stellar density scaled by the cluster's central value, R_{GC} is the radius of the cluster core, $r' = r/R_{\text{GC}}$, and we have assumed that the BHs cluster in the center. As seen, in this simple model we find that $\Gamma \propto N_{\text{BH}}m_{\text{BH}}^{1/2} \propto (N_{\text{BH}}m_{\text{BH}})m_{\text{BH}}^{-1/2}$. Therefore, if the number of BHs is kept fixed, $\Gamma \propto m_{\text{BH}}^{1/2}$, whereas if the total mass of BHs is kept fixed, $\Gamma \propto m_{\text{BH}}^{-1/2}$.

We can now use Equation (6) to provide an estimate for the rate of microlensing events in ωCen . For this we take $N_{\text{BH}} = 10^4$, $m_{\text{BH}} = 10 M_\odot$ (Zocchi et al. 2019),

$n_0 = 5 \times 10^4 \text{ pc}^{-3}$ (Noyola et al. 2008; D’Souza and Rix 2013), $v_0 = 25 \text{ km s}^{-1}$ (Sollima et al. 2009; Noyola et al. 2010), $R_{GC} = 3.25 \text{ pc}$ (Trager et al. 1995; Harris 2010), the observable threshold of μ to be $\mu_{\text{obs}} = 1.01$ (Bellini et al. 2017), $\int n' \sqrt{r'} dr' = 1$ (this integral is ≈ 1 for most relevant astrophysical profiles), and find $\Gamma \approx 0.2 \text{ yr}^{-1}$. This rate is promising and serves as our motivation for exploring this problem in greater detail. We continue below with a more accurate numerical approach.

3. Lensing Rate for Omega Centauri

Having motivated our lensing study of ωCen in Section 2 using analytical arguments, we now move on to a more accurate model using MC techniques. Below, we first describe our model of the stars and BHs in ωCen , after which we present our MC approach and corresponding results.

3.1. Cluster Model

Studies of stellar kinematics hint that ωCen is likely to harbor a population of BHs with a total mass of $\sim 10^5 M_\odot$ (Zocchi et al. 2019); however, the BH mass spectrum and distribution are not well constrained. Therefore, to keep our study as model independent as possible, we adopt the simple “energy equipartition” model from Kocsis et al. (2006) to describe the radial position and velocity distributions of the BHs, although we note that GCs likely never acquire perfect equipartition (e.g., Trenti & van der Marel 2013). In addition, we focus on modeling the microlensing rate from a BH population with a single mass m_{BH} to isolate the mass dependence on our results. Following Kocsis et al. (2006), the BHs uniformly distribute within a sphere of radius

$$R_{\text{BH}} = R_{\text{GC}} \sqrt{\langle m \rangle / m_{\text{BH}}} \quad (7)$$

with a corresponding velocity dispersion of

$$\sigma_{\text{BH}} = \sigma_{\text{GC}} \sqrt{\langle m \rangle / m_{\text{BH}}}, \quad (8)$$

where $\sigma_{\text{GC}} \approx \sqrt{(3/5)GM_{\text{GC}}/R_{\text{GC}}}$, M_{GC} and R_{GC} are the mass and radius of the cluster core, respectively, and $\langle m \rangle$ is the mean mass of the GC objects (stars + BHs).

In contrast to the BH population, the stellar distribution in ωCen is well constrained from observations. In this study we use the inferred stellar density and velocity dispersion profiles from D’Souza and Rix (2013) and Sollima et al. (2009), respectively. The former work suggests that the total core mass of ωCen is $M_{\text{GC}} = 5 \times 10^5 M_\odot$.

3.2. Monte Carlo Method

With the two distribution models for the BHs and stars presented above, we are now in a position to derive the expected microlensing rate for ωCen . For this, we developed an MC code that operates in the following way.

We first generate a BH assuming that it follows a circular orbit around the center of the core. The inclination angle of the orbit with respect to the LOS is randomized uniformly while the orbital radius and velocity are chosen according to Equations (7) and (8), respectively. Next, we generate a star whose position and velocity are chosen from the observationally inferred radial density and velocity dispersion profiles, as described in Section 3.1. At each time step in the BH’s orbit, we then estimate the microlensing magnification μ of the star

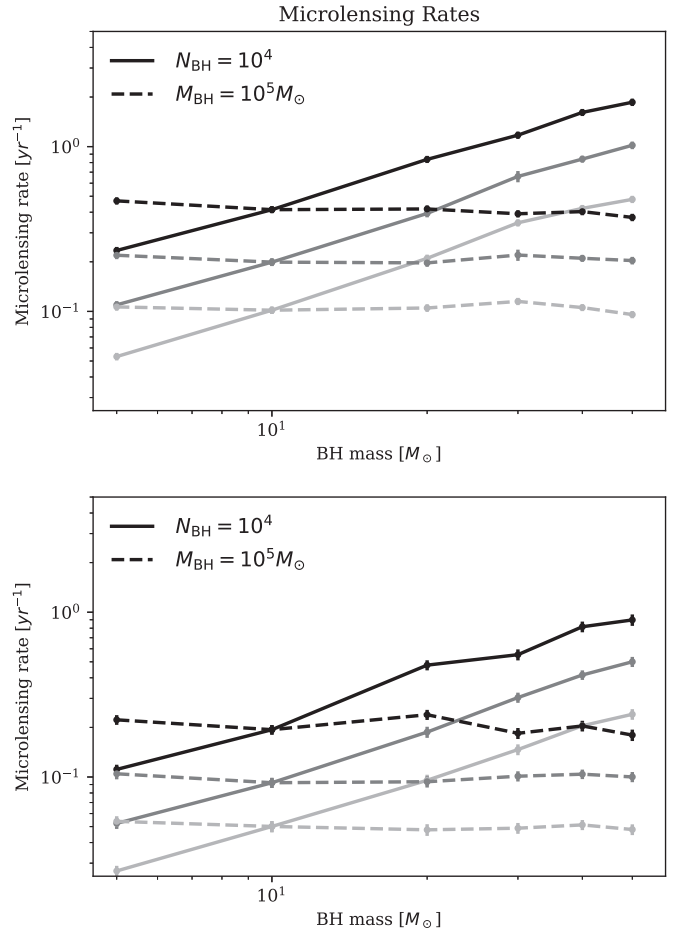


Figure 2. Event rates of cluster stars being microlensed by a corresponding population of cluster BHs in ωCen . The rates shown are estimated using MC techniques as described in Section 3.2, where the stars and BHs are distributed according to the models outlined in Section 3.1. The rates in the top and bottom panels are obtained using magnification thresholds of $\mu_{\text{obs}} = 1.01$ and $\mu_{\text{obs}} = 1.1$, respectively. The black, dark gray, and light gray lines show results for BH distributions with a radial size of $\{1/2, 1, 2\} \times R_{\text{BH}}$ from Equation (7), respectively. The solid and dashed lines show results for when the total number, N_{BH} , and total mass, M_{BH} , of the BHs are held fixed at $N_{\text{BH}} = 10^4$ and $M_{\text{BH}} = 10^5 M_\odot$, respectively. Results are discussed in Section 3.3.

and store its maximum value, μ_{max} . This entire process is repeated until a representative sample of star and BH pairs has been simulated. The final rate can then be calculated by counting the total number of microlensing events per unit time with $\mu_{\text{max}} > \mu_{\text{obs}}$, where μ_{obs} is the observational threshold. For the total rate calculation, we assume a total of 3×10^6 visible stars in the GC. Our simulation also calculates the duration of the lensing events. Beginning at the maximum brightness magnification, it records the magnification at each subsequent time step. From this brightness versus time data, we calculate the minimum time required for the magnification to decrease by the value $\mu_{\text{obs}} - 1$, which we define as the event duration. We find that events typically last on the order of several weeks.

3.3. Results

Microlensing rates for ωCen derived using our MC simulations described in Sections 3.1 and 3.2 are shown in Figure 2. The solid and dashed lines show results for when the

total number, N_{BH} , and total mass, M_{BH} , of the BHs are held fixed, respectively. To illustrate the dependence of our results on the uncertain scale of the radial distribution of the BHs, R_{BH} , we further show, in differently shaded lines, results for when R_{BH} is varied by a factor of 2 from its fiducial value given by Equation (7). An important parameter is the magnification threshold μ_{obs} , defined as the minimum value of μ (see (1)) associated with an observable brightness magnification. As seen in Figure 8 of Bellini et al. (2017), the photometric error is smaller for brighter stars, so the magnification threshold is also smaller for brighter stars. Since we cannot calculate this value for each individual star, we use two different threshold values for the cluster. From Figure 8 of Bellini et al. (2017), a standard error of 0.1 mag is conservative, as almost all stars have standard errors smaller than this. This leads to our conservative threshold of $\mu_{\text{obs}} = 1.1$. We also calculate the rate for $\mu_{\text{obs}} = 1.01$, equivalent to a standard error of 0.01 mag. Note that this is approximately the median standard error from Figure 8.

As seen, our numerical results indicate that the expected microlensing rate is in the range $0.1\text{--}1\text{ yr}^{-1}$ for ωCen , which is in good agreement with our analytical results from Section 2. For the constant BH number scenario the rate increases slightly faster than $m_{\text{BH}}^{1/2}$, and for the constant total BH mass scenario it decreases slower than $m_{\text{BH}}^{-1/2}$. These behaviors can be explained by the localization of the massive BHs closer to the cluster's center where the star density and, consequently, lensing rate are higher.

4. Discussion

Is there a significant population of BHs currently residing in GCs throughout our local volume? That is one of the current major questions in the rising field of GW astrophysics, where merging BHs, but not their origins, are directly observed. As suggested by both theory (e.g., Morscher et al. 2015; Rodriguez et al. 2016a) and observations (e.g., Askar et al. 2018; Kremer et al. 2018; Weatherford et al. 2019; Zocchi et al. 2019), GCs are likely able to retain a nonnegligible number of BHs, but direct evidence for BHs in GCs in the upper mass range observed by Advanced LIGO and Advanced Virgo ($\sim 30 M_{\odot}$) is still lacking.

In this Letter we have explored the possibility for constraining BH populations in GCs through the use of gravitational microlensing. We find it possible to detect BHs in the core of ωCen using microlensing observations with an expected rate range of $\sim 0.1\text{--}1\text{ yr}^{-1}$. This rate, each individual lensing lightcurve, and the spatial location of the lensed stars all depend on the BH mass spectrum and distribution. Hence, detections or nondetections of microlensing events can be used to constrain these quantities, although this is not trivial (e.g., Paczynski 1994; Udalski et al. 1994). Furthermore, while we are concerned only with microlensing events in which a BH acts as the lens for a cluster star, it is also possible for another cluster star to serve as the lens. Observationally, these two cases are distinguishable. A star lens can be observed optically while a BH lensing event is characterized by an unobservable lens.

This strategy described in this Letter is naturally not limited to ωCen , but can be applied to any of the ~ 150 GCs in the MW. However, it is important to keep in mind that ωCen is a unique GC that likely has an unusually high microlensing rate. ωCen has a greater mass than other Galactic GCs (e.g.,

Baumgardt & Hilker 2018), and has even been proposed to be a tidally stripped dwarf galaxy (Majewski et al. 2000; Ibata et al. 2019). Additionally, it cannot be assumed that all GCs contain as many BHs as ωCen . However, several clusters analyzed in recent works likely contain hundreds of BHs and, therefore, may have significant microlensing rates (Arca Sedda et al. 2018; Askar et al. 2018; Kremer et al. 2018; Weatherford et al. 2019).

Observing BH microlensing events in GCs is challenging, but will likely soon become possible as telescopes with improved performance continue to be constructed. This includes both ground-based telescopes, such as the Thirty Meter Telescope, and space-based ones, such as The Wide Field Infrared Survey Telescope. Past studies of data from the Hubble Space Telescope have already been used to analyze microlensing events near the galactic center and have successfully constrained lens masses (e.g., Kains et al. 2017). Determining the mass of GC BHs may be more difficult as the source and lens distances are similar and, therefore, must be measured precisely. Our simulations suggest that microlensing events last on the order of several weeks. Therefore, observing the cluster on the order of once every few days should provide sufficient data to capture most lensing events. Even though resolution continues to improve, observations near the GC core center may still face the issue of crowding, in which it is impossible to resolve two nearby stars. In this case, lensing will still be observable, but since the localization of the lensed stars can be ambiguous, the uncertainty of the inferred BH population parameters will be higher. In follow-up work we will study how to optimize current and future search strategies for observing such BH microlensing events.

The authors thank Noé Kains for discussions. The authors appreciate the generous support of Columbia University in the City of New York and the University of Florida. J.Z. is grateful for support from the Ng Teng Fong Student Internship Fund administered through the Columbia College Summer Fund. J.S. acknowledges support from the Lyman Spitzer Fellowship, and funding from the European Union's Horizon 2020 research and innovation programme under the Marie Skłodowska-Curie grant agreement No. 844629. D.V. is grateful to the Ph.D. grant of the Fulbright foreign student program.

ORCID iDs

Doğa Veske  <https://orcid.org/0000-0003-4225-0895>

Imre Bartos  <https://orcid.org/0000-0001-5607-3637>

Szabolcs Márka  <https://orcid.org/0000-0002-3957-1324>

References

- Aasi, J., Abbott, B. P., Abbott, R., et al. 2015, *CQGra*, **32**, 074001
 Abbott, B. P., Abbott, R., Abbott, T. D., et al. 2016a, *PhRvL*, **116**, 061102
 Abbott, B. P., Abbott, R., Abbott, T. D., et al. 2016b, *PhRvL*, **116**, 241103
 Abbott, B. P., Abbott, R., Abbott, T. D., et al. 2016c, *PhRvX*, **6**, 041015
 Abbott, B. P., Abbott, R., Abbott, T. D., et al. 2017a, *PhRvL*, **118**, 221101
 Abbott, B. P., Abbott, R., Abbott, T. D., et al. 2017b, *PhRvL*, **119**, 141101
 Acernese, F., Agathos, M., Agatsuma, K., et al. 2015, *CQGra*, **32**, 024001
 Antonini, F., & Gieles, M. 2020, *MNRAS*, **492**, 2936
 Antonini, F., & Rasio, F. A. 2016, *ApJ*, **831**, 187
 Arca Sedda, M., Askar, A., & Giersz, M. 2018, *MNRAS*, **479**, 4652
 Askar, A., Arca Sedda, M., & Giersz, M. 2018, *MNRAS*, **478**, 1844
 Askar, A., Szkudlarek, M., Gondke-Rosińska, D., Giersz, M., & Bulik, T. 2017, *MNRAS*, **464**, L36
 Banerjee, S., Baumgardt, H., & Kroupa, P. 2010, *MNRAS*, **402**, 371
 Bartos, I., Kocsis, B., Haiman, Z., & Márka, S. 2017, *ApJ*, **835**, 165

- Baumgardt, H., & Hilker, M. 2018, *MNRAS*, 478, 1520
- Belczynski, K., Repetto, S., Holz, D. E., et al. 2016, *ApJ*, 819, 108
- Bellini, A., Anderson, J., Bedin, L. R., et al. 2017, *ApJ*, 842, 6
- Bennett, D. P., Becker, A. C., Quinn, J. L., et al. 2002, *ApJ*, 579, 639
- Brassington, N. J., Fabbiano, G., Blake, S., et al. 2010, *ApJ*, 725, 1805
- Chomiuk, L., Strader, J., Maccarone, T. J., et al. 2013, *ApJ*, 777, 69
- Di Carlo, U. N., Giacobbo, N., Mapelli, M., et al. 2019, *MNRAS*, 487, 2947
- Dominik, M., Belczynski, K., Fryer, C., et al. 2012, *ApJ*, 759, 52
- D'Souza, R., & Rix, H.-W. 2013, *MNRAS*, 429, 1887
- Fragione, G., Grishin, E., Leigh, N. W. C., Perets, H. B., & Perna, R. 2019, *MNRAS*, 488, 47
- Fragione, G., & Kocsis, B. 2018, *PhRvL*, 121, 161103
- Giacobbo, N., & Mapelli, M. 2018, *MNRAS*, 480, 2011
- Giesers, B., Dreizler, S., Husser, T.-O., et al. 2018, *MNRAS*, 475, L15
- Giesers, B., Kamann, S., Dreizler, S., et al. 2019, *A&A*, 632, A3
- Gültekin, K., Miller, M. C., & Hamilton, D. P. 2006, *ApJ*, 640, 156
- Hamers, A. S., Bar-Or, B., Petrovich, C., & Antonini, F. 2018, *ApJ*, 865, 2
- Harris, W. E. 2010, arXiv:1012.3224
- Hong, J., & Lee, H. M. 2015, *MNRAS*, 448, 754
- Ibata, R. A., Bellazzini, M., Malhan, K., Martin, N., & Bianchini, P. 2019, *NatAs*, 3, 667
- Jetzer, P., Straessle, M., & Wandeler, U. 1998, *A&A*, 336, 411
- Kains, N., Calamida, A., Sahu, K. C., et al. 2017, *ApJ*, 843, 145
- Kocsis, B., Gáspár, M. E., & Márka, S. 2006, *ApJ*, 648, 411
- Kremer, K., Ye, C. S., Chatterjee, S., Rodriguez, C. L., & Rasio, F. A. 2018, *ApJL*, 855, L15
- Maccarone, T. J., Kundu, A., Zepf, S. E., & Rhode, K. L. 2007, *Natur*, 445, 183
- Maccarone, T. J., Kundu, A., Zepf, S. E., & Rhode, K. L. 2011, *MNRAS*, 410, 1655
- Majewski, S. R., Patterson, R. J., Dinescu, D. I., et al. 2000, *LIACo*, 35, 619
- Mapelli, M. 2016, *MNRAS*, 459, 3432
- Mapelli, M., Giacobbo, N., Ripamonti, E., & Spera, M. 2017, *MNRAS*, 472, 2422
- McKernan, B., Ford, K. E. S., Bellovary, J., et al. 2018, *ApJ*, 866, 66
- Miller-Jones, J. C. A., Strader, J., Heinke, C. O., et al. 2015, *MNRAS*, 453, 3918
- Morscher, M., Pattabiraman, B., Rodriguez, C., Rasio, F. A., & Umbreit, S. 2015, *ApJ*, 800, 9
- Murguía-Berthier, A., MacLeod, M., Ramirez-Ruiz, E., Antoni, A., & Macias, P. 2017, *ApJ*, 845, 173
- Noyola, E., Gebhardt, K., & Bergmann, M. 2008, *ApJ*, 676, 1008
- Noyola, E., Gebhardt, K., Kissler-Patig, M., et al. 2010, *ApJL*, 719, L60
- O'Leary, R. M., Kocsis, B., & Loeb, A. 2009, *MNRAS*, 395, 2127
- Paczynski, B. 1986, *ApJ*, 304, 1
- Paczynski, B. 1994, *AcA*, 44, 235
- Park, D., Kim, C., Lee, H. M., Bae, Y.-B., & Belczynski, K. 2017, *MNRAS*, 469, 4665
- Pietrukowicz, P., Minniti, D., Jetzer, P., Alonso-García, J., & Udalski, A. 2012, *ApJL*, 744, L18
- Portegies Zwart, S. F., & McMillan, S. L. W. 2000, *ApJL*, 528, L17
- Rhoads, J. E., & Malhotra, S. 1998, *ApJL*, 495, L55
- Rodriguez, C. L., & Antonini, F. 2018, *ApJ*, 863, 7
- Rodriguez, C. L., Chatterjee, S., & Rasio, F. A. 2016a, *PhRvD*, 93, 084029
- Rodriguez, C. L., Zevin, M., Pankow, C., Kalogera, V., & Rasio, F. A. 2016b, *ApJL*, 832, L2
- Romero-Shaw, I. M., Lasky, P. D., & Thrane, E. 2019, *MNRAS*, 490, 5210
- Safonova, M., & Stalin, C. S. 2010, *NewA*, 15, 450
- Sahu, K. C., Casertano, S., Livio, M., et al. 2001, *Natur*, 411, 1022
- Samsing, J. 2018, *PhRvD*, 97, 103014
- Samsing, J., Askar, A., & Giersz, M. 2018a, *ApJ*, 855, 124
- Samsing, J., D'Orazio, D. J., Kremer, K., Rodriguez, C. L., & Askar, A. 2019, arXiv:1907.11231
- Samsing, J., & Ilan, T. 2018, *MNRAS*, 476, 1548
- Samsing, J., & Ilan, T. 2019, *MNRAS*, 482, 30
- Samsing, J., MacLeod, M., & Ramirez-Ruiz, E. 2014, *ApJ*, 784, 71
- Samsing, J., MacLeod, M., & Ramirez-Ruiz, E. 2018b, *ApJ*, 853, 140
- Samsing, J., & Ramirez-Ruiz, E. 2017, *ApJL*, 840, L14
- Schröder, S. L., Batta, A., & Ramirez-Ruiz, E. 2018, *ApJL*, 862, L3
- Shih, I. C., Kundu, A., Maccarone, T. J., Zepf, S. E., & Joseph, T. D. 2010, *ApJ*, 721, 323
- Silber, K., & Tremaine, S. 2017, *ApJ*, 836, 39
- Sollima, A., Bellazzini, M., Smart, R. L., et al. 2009, *MNRAS*, 396, 2183
- Spera, M., Mapelli, M., Giacobbo, N., et al. 2019, *MNRAS*, 485, 889
- Stephan, A. P., Naoz, S., Ghez, A. M., et al. 2016, *MNRAS*, 460, 3494
- Stone, N. C., Metzger, B. D., & Haiman, Z. 2017, *MNRAS*, 464, 946
- Strader, J., Chomiuk, L., Maccarone, T. J., Miller-Jones, J. C. A., & Seth, A. C. 2012, *Natur*, 490, 71
- Trager, S. C., King, I. R., & Djorgovski, S. 1995, *AJ*, 109, 218
- Trenti, M., & van der Marel, R. 2013, *MNRAS*, 435, 3272
- Udalski, A., Szymanski, M., Stanek, K. Z., et al. 1994, *AcA*, 44, 165
- VanLandingham, J. H., Miller, M. C., Hamilton, D. P., & Richardson, D. C. 2016, *ApJ*, 828, 77
- Venumadhav, T., Zackay, B., Roulet, J., Dai, L., & Zaldarriaga, M. 2019, arXiv:1904.07214
- Weatherford, N. C., Chatterjee, S., Kremer, K., & Rasio, F. A. 2019, arXiv:1911.09125
- Yang, Y., Bartos, I., Gayathri, V., et al. 2019, *PhRvL*, 123, 181101
- Zackay, B., Venumadhav, T., Dai, L., Roulet, J., & Zaldarriaga, M. 2019, *PhRvD*, 100, 023007
- Zevin, M., Pankow, C., Rodriguez, C. L., et al. 2017, *ApJ*, 846, 82
- Zevin, M., Samsing, J., Rodriguez, C., Haster, C.-J., & Ramirez-Ruiz, E. 2019, *ApJ*, 871, 91
- Ziosi, B. M., Mapelli, M., Branchesi, M., & Tormen, G. 2014, *MNRAS*, 441, 3703
- Zocchi, A., Gieles, M., & Hénault-Brunet, V. 2019, *MNRAS*, 482, 4713